Beilstein-Institut

Towards Electron Beam Induced Deposition Improvements for Nanotechnology

Johannes J.L. Mulders[1,*] and Aurelien Botman[2]

[1]FEI Electron Optics, Achtseweg Noord 5, 5600 KA Eindhoven, The Netherlands

[2]FEI Company, 5350 NE Dawson Creek Drive, Hillsboro, OR 97124, U.S.A.

E-Mail: *jjm@fei.com

Abstract

Electron beam induced deposition can be applied as a direct write technique for the creation of 3 dimensional nano-scale structures. The technique does not require lift-off and mask based process steps and therefore has potential for application in rapid prototyping for nano-technology, with a high degree of flexibility. The material quality and microstructure of the deposition however, is usually somewhat differ-ent to that of the pure material and hence the obtained properties of the nano-depositions do not reflect the bulk properties of the desired ma-terial. Current research is focused on improvements for the deposition processes with the aim to improve the purity of the deposition to such an extent that the local characteristic aimed for (such as conductivity) is good enough to attain the required local functionality. This paper reports on the current status and on some of the methods that have been applied to improve the deposition process.

Introduction

Electron beam induced deposition (EBID) is a technique that can be used for the direct creation of nanoscale structures in 3 dimensions. The base technique includes a scanning electron microscope (SEM) equipped with a gas supply line providing precursor molecules released in the vacuum chamber of the SEM and close to the substrate. These molecules will

temporarily adhere to the surface and within that residence time they may interact with electrons supplied by the electron beam (Figure 1 shows a schematic representation of the process).
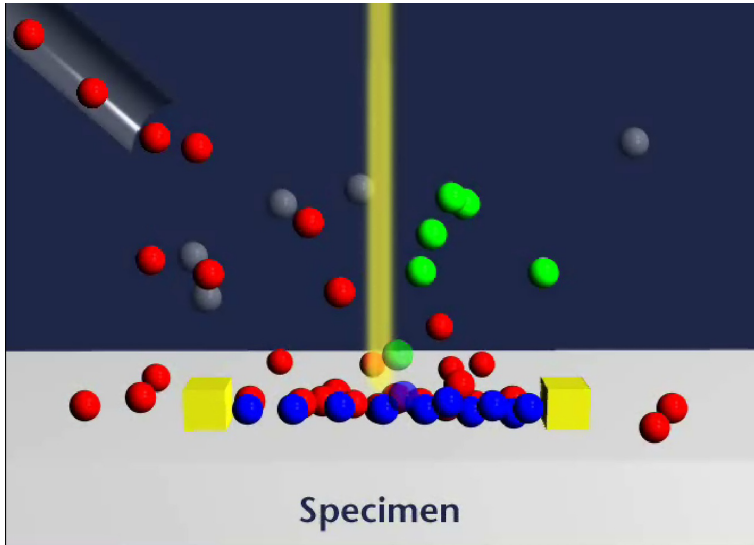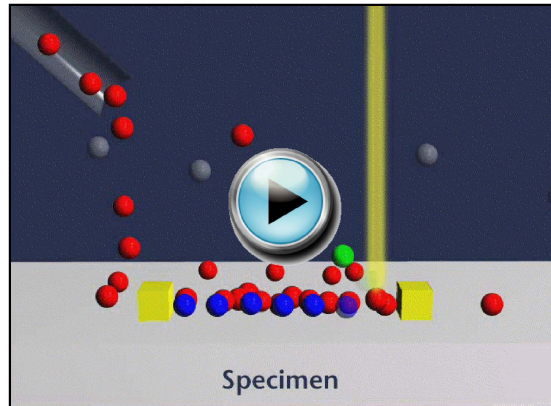

Figure 1. Schematic representation of the EBID process: Precursor molecules (red) are decomposed by interaction with the electron beam into a volatile (green) and non-volatile (blue) part. By beam patterning a conductive pad is created between the two contact pads (yellow).

Movie. Principle of EBID process

This interaction results in a decomposition of the precursor molecule into a volatile part such as a CO or a CH_4 group (that is pumped away by the vacuum system) and a non-volatile part such as the metal of interest that forms a very local deposition on the substrate. Typically the

local flux of molecules in the order of 10^{16} mol/cm^2.s, while beam currents are in the range 50 pA to 1 nA. It is generally assumed that the secondary electrons with an energy < 50 eV, emitted from the substrate, are the main contributors to the decomposition process. An example of a pattern deposited using $W(CO)_6$ as a precursor is shown in Figure 2.
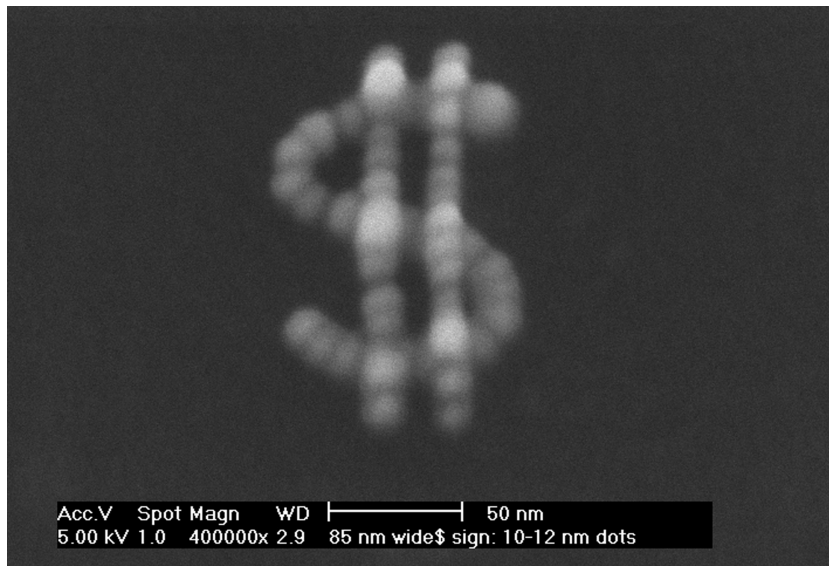

Figure 2. Example of an EBID created dollar symbol, showing the direct nano-patterning capability. The image shows nano-dots of $10 - 12$ nm made by the decomposition of $W(CO)_6$ by the electron beam exposure at 3 seconds per point and a total production time of 150 seconds.

Typically for the creation of metallic structures the precursor is an organo-metallic chemical, the vapour of which is used as a gas supply to the system. Many of these chemicals are used in CVD based processes, where decomposition is driven by collisions with the substrate at high temperature (thermal decomposition). Examples of precursor materials that are regularly used for EBID by many users across the world are listed in Table 1.

Table 1. Overview of commonly used precursors for electron beam induced deposition

Precursor	Short name / formula	For deposition of
methyl cyclo-pentadienyl platinum trimethyl	MeCpPtMe$_3$	Platinum
tungsten hexacarbonyl	W(CO)$_6$	Tungsten
naphthalene	C$_{10}$H$_8$	Carbon
cobalt octacarbonyl	Co$_2$(CO)$_8$	Cobalt
tetra ethyl ortho silicate	TEOS	SiO$_x$
dimethyl gold acetyl acetonate	Me$_2$Auacac	Gold

Applications for these materials range from contacting nanotubes and nanowires (conductivity, work function), seeding for nanowire growth, electrical isolation, optical and chemical activity and nanoscale magnetic structures such as for domain wall movement or tips for Magnetic Force Microscopy (MFM). It should be noted that the precursors listed in Table 1 all contain carbon atoms in some form (methyl, carbonyl groups) and ideally the decomposition reaction should only decompose into non-volatile (metal) and volatile products such as CO. For example, ideally the creation of nanoscale tungsten depositions should be close to the following reaction:

$$W(CO)_6 + \text{electrons} \quad \rightarrow \quad W \downarrow \quad + \quad 6 \, CO \uparrow + \text{electrons}$$

In practice however, the decomposition is not 100% effective and hence there is a co-deposition of both carbon and oxygen, together with the tungsten. Typically for the process described above, the elements present in the deposition are: W 37 at%, O 27 at% and C 36 at%. For this reason the local conductivity of the structure will deviate substantially from the value for bulk tungsten. This applies to any relevant characteristic of the deposition: the local nanoscale property is generally quite different from the known bulk property due to the presence of undesired elements. Therefore current research focuses on a better understanding of the fundamental processes [1, 2], optimization of the basic parameters [3], additional *ex situ* purification techniques [4] and the application of other, carbon free precursors [5]. In this paper the purification of platinum depositions is discussed as well as the use of alternative (non-standard) precursors for platinum and gold and an outlook into further improvements and new materials.

CURRENT STATUS OF THE TECHNOLOGY

In literature it is found that the number of publications on the subject of EBID is increasing and a wide range of materials and processes have been tried [6]. The basic processes of the technique, such as the individual cross-section for the reaction of energetic electrons with adsorbed molecules is in its infancy and is sometimes studied by looking at reaction products (RGA) and X-ray photo-electron spectroscopy (XPS) *in situ*, when the adsorbed precursor is irradiated with an electron broad beam. These techniques have a sensitivity that is not adequate for the small amount of material involved when performing EBID at nanoscale, but for a broad and low energy electron beam producing a thin film, they are well suited. From these measurements it can be derived how the material decomposes and how reaction products are formed. Also the actual growth dynamics have now been simulated by computer models [7] and the basic growth parameters are increasingly better understood. Overall the research focuses on understanding the basic reaction mechanisms, both from a chemical point of view and from a dynamic point of view. In addition many methods are investigated to get a better purity with minimal or no changes of the 3 dimensional shape.

One thing which is very clear from literature is that the total parameter space is very large and, more importantly, not all parameters are listed when experimental results are presented. As a consequence the reproducibility of results is poor. The main reason for this is a non-consistent approach from user to user and from tool to tool, indicating the presence of one or more process parameters that have not yet been recognized. As an example of one of these parameters, it has been observed through recent experiments, that the vacuum and cleanliness conditions are quite crucial for the results. This is because the processes involved include real surface reactions with low amounts of material and hence any molecules that may be present can add to the process. Vacuum conditions are generally not reported in literature. Even the exact procedure used by the SEM operator may come to influence the process, due to a lack of awareness of all the critical factors involved in good experimental reproducibility. When performing EBID experiments it is highly recommended for an operator to apply the following conditions:

1) Related to the chamber vacuum:

  a) waiting until the base vacuum of the system is at least $< 4 \times 10^{-6}$ mbar;

  b) minimizing the amount of residual water vapour by using a cold finger or an overnight pump out;

  c) controlling residual hydrocarbons by working in very clean conditions and by applying a regular plasma clean of the chamber;

  d) regularly confirming that the Penning gauge readout is correct: EBID processes tend to increase the contamination of the interior of the Penning indicating the pressure to be better than in reality.

2) Related to sample mounting:

  a) not using double-sided adhesive carbon tabs;

  b) not using silver paint or carbon paint;

  c) being suspicious to any part which might produce additional out-gassing, such as plastics or other non-vacuum compatible materials;

  d) using a clamping mechanism to fix the sample to the holder instead.

3) Related to sample holders:

  a) not using gel packs;

  b) not using membrane packs;

  c) using a single, clean container for each individual sample (Teflon or glass);

  d) placing a clear marker (*e.g.* using a Focused Ion Beam) on the sample for later locating the small deposited material (for example for AFM measurements).

Ideally the sample surface should be well defined (material type and crystal orientation) and the vacuum should be quantified with more data than just the pressure readout: a mass spectrometer spectrum can provide more informative and detailed data about the actual vacuum present during the experiment.

RECENT PROGRESS ON PURIFICATION OF PLATINUM

For platinum the most widely used precursor is $MeCpPtMe_3$, mostly used for contacting nanotubes and nanowires. The challenge in improving the EBID process for platinum starts with an analysis of the main system parameters that have an influence on the actual composition. These refer to beam energy and beam current. The relation between the amount of platinum as determined by low kV EDX, as a function of beam current and energy is shown in Figure 3. As beam current and beam energy together define the power of the beam it is also interesting to plot the power against the platinum content, as shown in Figure 4.
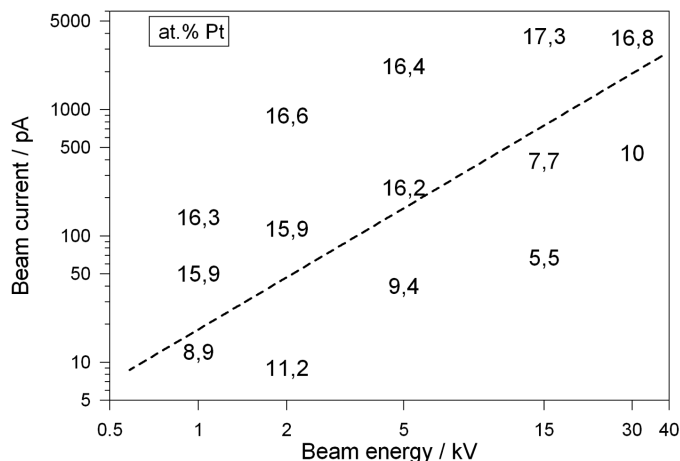

Figure 3. The amount of Pt given in numbers as atomic% (at%) as a function of the applied beam energy and beam current. The dashed line splits the parameter space into two regions: ~16 at% and < 16 at% [8].
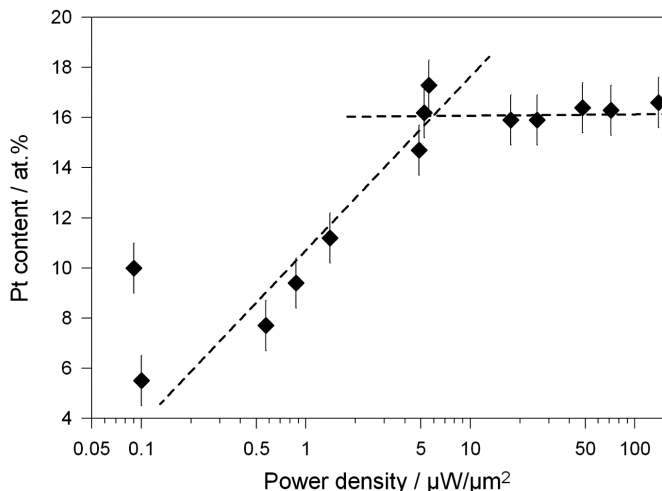
Figure 4. Same data as in Figure 3, but now expressed as a function of the beam power density, defined here as the beam current × beam energy/projected electron interaction area on the substrate surface as derived from Monte Carlo simulations [8].

From both figures it can be concluded that:

1. The higher the power density, the higher the amount of platinum. It is suggested that additional heat generation during the deposition process may deliver extra energy and hence enhance the decomposition, as is also suggested for decomposition of cobalt [9].

2. There appears to be an upper limit of purity around 16 at% Pt. This suggests a decomposition where 4 CH_4 groups are removed from the $MeCpPtMe_3$, leaving the remaining pentadienyl ring bound to the platinum. The reaction could then be proposed as follows:

$$C_9H_{16}Pt + \text{electrons} \rightarrow 4\,CH_4 \uparrow + C_5Pt \downarrow + \text{electrons}$$

resulting in 1 Pt atom out of 6 per deposited molecule, i.e. 16 at%.

A further improvement could be obtained by post treatment of the deposition:

1. Annealing in oxygen [4]: this results in 70 at% Pt when applied in the temperature range $250 - 500°C$ and is generally attributed to a burn-off of the carbon content and the release of CO or CO_2.

2. Annealing in a hydrogen radical environment [10]: this results in an improvement of the platinum content to 35 at% in the temperature interval $150 - 180°C$. At higher temperatures no further changes have been observed, but it is remarkable that the improvement starts at a lower temperature, most likely by the generation of CH_4.

Although the improvement in the relative amount of Pt is clear it should be noted that with these treatments the substrate will be subjected to a relative high temperature (not always desirable for the sample as a whole). In consequence the shape of the deposited material can change quite a lot, due to the violent and non-symmetric removal of material.

Another way to create Pt depositions is to use a non-organic precursor $Pt(PF_3)_4$ [11]. This precursor contains PF_3 ligands and may therefore produce some fluorine-containing molecules during decomposition, such as F_2 or HF. The sample should be resistant to these etching molecules. Quantitative measurements of small-sized depositions using the standard EDX technique is not straightforward because the $PtM\alpha_1$ X-ray line at 2.05 keV is very close to the $PK\alpha$ line at 2.013 keV and hence these lines cannot be very well distinguished by the EDX system, which typically has an energy resolution of around 120 eV. In comparative analysis one can either use the combined X-ray peak or use TEM or WDX at higher energy for analysis of the PtL lines.

Similar to the $MeCpPtMe_3$ precursor, post processing can be applied to improve the purity. It should be noted that for platinum the main application is focused on electrical conductivity and hence the specific resistivity ($\mu\Omega.cm$) is the parameter of interest and this can be measured by using a 4 point probe test structure as shown in Figure 5. In this typical structure the resistivity can be measured without influence of the contact resistance and by measuring the cross section the resistivity can be calculated.
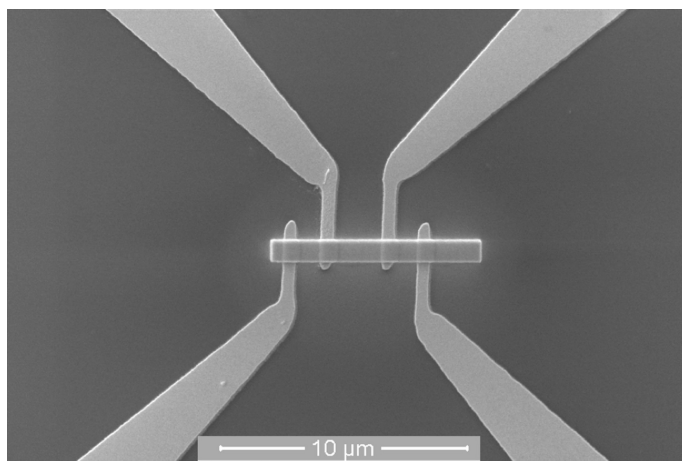

Figure 5. A 4 point probe test structure used to measure the resistance across an EBID strip. By measuring the height of the strip the cross-section can be determined and hence the material resistivity. The end of the strip can also be used for compositional measurement using EDX without affecting the portion of the strip used for resistivity determination.

Although the composition and purity of the deposition plays a dominant role in the final electrical property of the material, it should also be noted that the local fine structure (grain size) and crystalline distribution also contribute to the final result. These can be determined by TEM based analysis and often reveal small pure Pt grains embedded in a matrix containing the other elements such as C for $MeCpPtMe_3$ or P and O for $Pt(PF_3)_4$. All improvements that have been obtained for platinum depositions can best be summarized by looking at the progress in the decrease of the deposited material resistivity, as shown in Figure 6. From this figure it is obvious that much progress has been made by the various methods and post processing and that the conductivity is now so close to the value for bulk Pt, that the EBID process may become useful for the application it was intended for (such as nano-contacts).
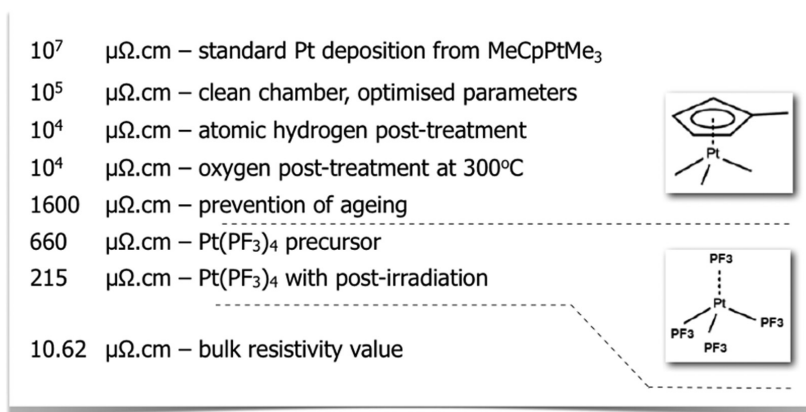

Figure 6. Substantial improvements in the specific resistivity for EBID Pt, using a variety of purification methods and/or a non-organic precursor [8].

RECENT PROGRESS ON PURIFICATION OF GOLD

The interest in gold for nano-depositions is driven by its use as a nanoseed for growing of III/V semiconductor nanowires, as an optical active medium for plasmonic structures and as a marker and binding site for biological structures. In addition it also can be used for creating electrical contacts. The most commonly applied precursor is $Me_2Au(acac)$ and this precursor can indeed be used for EBID but the amount of Au is only $8-10\,at\%$ with the remainder being mainly C and a little O. Also for this precursor a post anneal step in a nitrogen environment is possible to improve the purity, as shown in Table 2.

Table 2. Composition (at%) of EBID from $Me_2Au(acac)$. Depositions made at room temperature. Anneal steps at 250 and 400˚C in a nitrogen environment. The anneal steps were carried out at ICFO, Barcelona Spain.

Element	Sample 1	Sample 2	Sample 3
	no anneal	250°C -3 hr	400°C -3 hr
C	79.1	78.9	54
O	11.4	11.6	20.4
Au	9.5	9.5	25.6
	100	100	100

More recently annealing was also applied in an oxygen environment, which is assumed to be more active for assisting the burn-off of the carbon [10] than a relatively inert environment of nitrogen would be. This is confirmed by the result shown in Figure 7. The carbon content at 400 ˚C drops to around 22 at% for anneal in oxygen, while for anneal in nitrogen the carbon content reduces to around 54 at%.
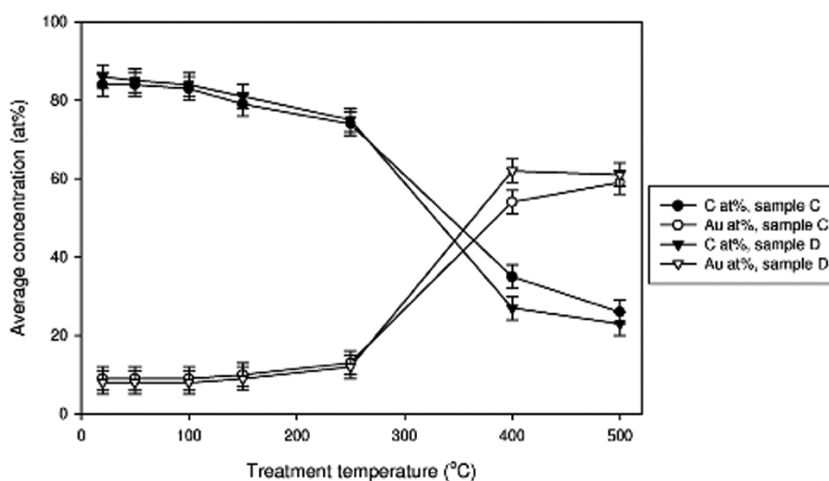

Figure 7. EBID using $Me_2Au(acac)$. The amount of gold (at%) as a function of the anneal temperature using an oxygen environment for 10 minutes. The curve shows a saturation level around 60 at%. This figure was first published in [10] and is reproduced with permission.

Although the results from both anneal steps are encouraging, it should be noted that the shape of the nano-deposit suffers. At even higher temperatures the Au may also coagulate and form larger isolated clusters on the substrate.

Application of a non-organic precursor $AuClPF_3$ is reported in literature [12] and this produces very high purity gold. However this precursor is not commercially available and not very stable (it decomposes spontaneously quite easily at room temperature). In addition

it releases fluorine during the deposition process which may attack the substrate, sample and/or the system. Therefore, recently a new precursor was tested: Au(CO)Cl. This material has been known since 1925 and is readily available. An actual deposition with this precursor is shown in Figure 8. A comparison of the purity of the gold deposition is shown in the spectra in Figure 9 for Me$_2$Au(acac) and Au(CO)Cl respectively. The quantitative purity is better than 92 at% [13], the yield is 6.5×10^{-4} μm^3/nC for 5 kV, 100 pA and in the gas limited regime. The deposition shows a grain structure. The yield is relatively low and this is due to the low gas flux. However, the gas flux cannot be increased by precursor heating due to enhanced spontaneous chemical decomposition.
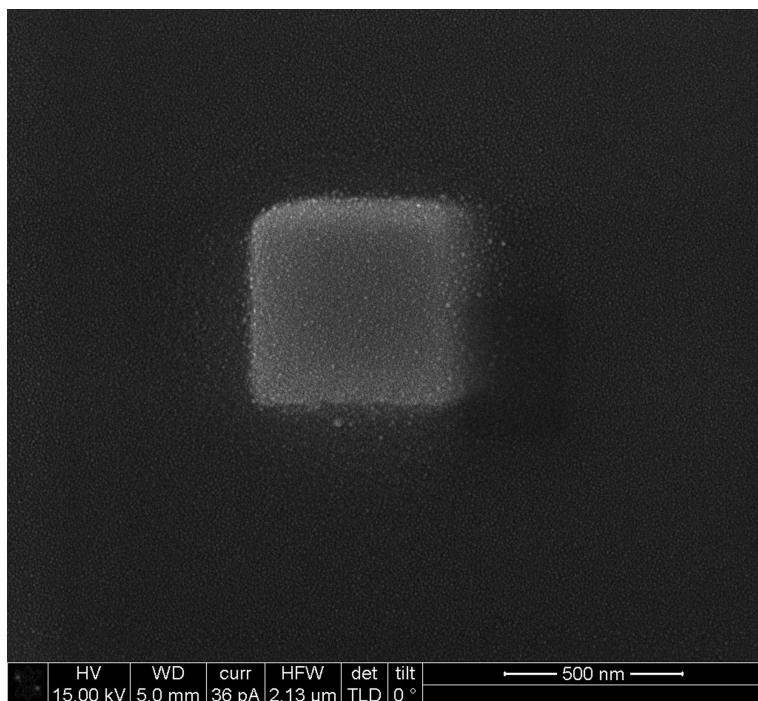

HV	WD	curr	HFW	det	tilt	⊢——— 500 nm ———⊣
15.00 kV	5.0 mm	36 pA	2.13 µm	TLD	0 °	

Figure 8. Deposition of a 500×500 nm pad at 15 kV, 25pA with 15 minutes total time.

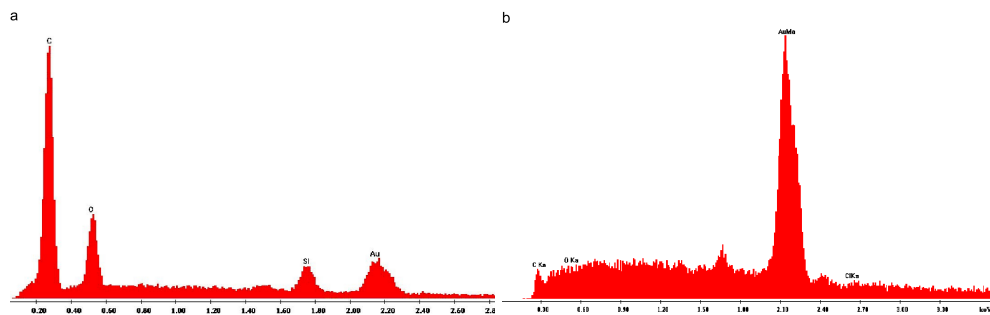The yield is relatively low, but the purity is very good.

Figure 9. (a) EDX spectrum comparison of EBID with Me2Au(acac) giving ~ 8 at% Au; **(b)** EBID with Au(CO)Cl giving > 92 at% Au.

The precursor Au(CO)Cl allows the production of very pure gold structures on substrates that are compatible with the release of some chlorine, such as SiO_2 and Si_3N_4. It also allows the creation of very small nanoscale dots as shown in Figure 10. It shows that the material has potential for application in plasmonic structures for the manipulation of light, using gold antennas at sub-wavelength dimensions.
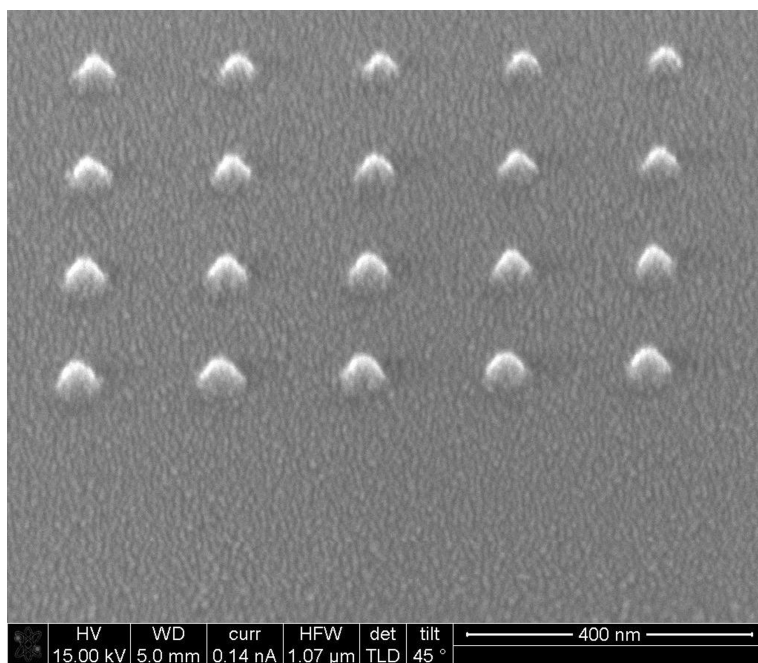

Figure 10. Part of a 15 × 15 dot array. Point depositions at 15 kV, 25 pA. Diameter 50 nm, height is around 40 nm. Each dot is high purity gold deposited from Au(CO)Cl. Production time of the total array is 5 minutes.

OUTLOOK AND DISCUSSION

As illustrated above, recent developments in the search for higher purity of the deposited material have resulted in substantially higher atomic content of the desired metal, both for Pt and for Au. Therefore application of these materials is now within reach of the nanotechnology scientist. Although the local property of interest is not yet at the level of the bulk material, the property gets very close to this and becomes practical for use. A second trend that is ongoing is the broadening of the materials range including magnetic materials such as Fe, Co and Ni. Co has been widely studied and has already been shown to exhibit ferromagnetic behaviour [3] and for Fe similar results are emerging. Other materials of interest might be Pd [14], and in view of the lessons learned for Pt these results can be expected to improve in the near future.

Finally it is interesting to observe the use of EBID together with other techniques where the advantages of both can be combined. One such opportunity is the combination of atomic layer deposition (ALD) with seeds made by EBID [15], both using the same MeCpPtMe$_3$ precursor, but now resulting in 100% Pt which is driven by the ALD process. It has been shown that the structural behaviour of EBID-seeded ALD growth provides the same purity and crystal structure (texture) as films grown by ALD alone. The combination of the two techniques also allows a higher total process speed, if the area to cover is relatively large: this is due to the fact that ALD is a parallel growth technique and the required EBID seeds can be very thin, on the order of 1 nm only.

REFERENCES

[1]   Smith, D.A., Fowlkes, J.D., Rack, P. D. (2007) *Nanotechnology* **18**:265308.
      doi: 10.1088/0957-4484/18/26/265308.

[2]   Wnuk, J.D., Gorham, J.M., Rosenberg, S.G., van Dorp, W.F., Madey, T.E., Hagen, C.W. and Fairbrother, D.H. (2010) *J. Vac. Sci. Technol.* **B** (in press).

[3]   Fernandez-Pacheco, A., De Teresa, J.M., Cordoba, R. and Ibarra, M.R. (2009) *J. Phys. D, Appl. Phys.* **42**:055005.

[4]   Botman, A., Mulders, J.J.L., Weemaes, R. and Mentink, S. (2006) *Nanotechnology* **17**: 3779 – 3785.
      doi: 10.1088/0957-4484/17/15/028.

[5]   Barry, J.D., Ervin, M., Molstad, J., Wickenden, A., Britlinger, T., Hoffmann, P. and Melngailis, J. (2006) *J. Vac. Sci. Technol.* B **24** (6):3165 – 68.
      doi: 10.1116/1.2395962.

[6]   Botman, A., Mulders, J.J.L. and Hagen, C.W. (2009) *Nanotechnology* **20**:372001.
doi: 10.1088/0957-4484/20/37/372001.

[7]   Rack, P.D., Fowlkes, J.D., Randolph, S.J., Smith, D.A. (2006) *First International Workshop on Electron Beam Induced deposition, Delft, The Netherlands,* 16 – 17.

[8]   Botman, A. (2009) *Thesis* TU Delft, ISBN 978 – 90 – 5335 – 240 – 3.

[9]   Córdoba, R., Sesé, J., De Teresa, J.M., Ibarra, M.R. (2009) *Microelectronic Engineering* **87**(5 – 8):1550 – 1553.

[10]   Botman, A., Hesselberth, M., and Mulders, J.J.L. (2008) *Microelectronic Engineering* **85**:1139 – 1142.
doi: 10.1016/j.mee.2007.12.036.

[11]   Barry, J.D., Ervin, M., Molstad, J., Wickenden, A., Britlinger, T., Hoffmann, P. and Melngailis, J. (2006) *J. Vac. Sci. Technol.* B, **24** (6):3165 – 68.
doi: 10.1116/1.2395962.

[12]   Hoffmann, P., Utke, I., Cicoira, F., Dwir, B., Leifer, K., Kapon, E. and Doppelt, P. (2000) *Mat. Res. Soc. Symp. Proc.* **624**:171.

[13]   Mulders, J.J.L., Botman, A. (2009) *Procedings Microscopy and MicroAnalysis* Richmond USA, 1126.

[14]   Spoddig, D., Schindler, K., Roediger, P., Barzola-Quiquia, J., Fritsch, K., Mulders, J. and Esquinazi, P. (2007) *Nanotechnology* **18**:495202
doi: 10.1088/0957-4484/18/49/495202.

[15]   Mackus, A.J.M., Mulders, J.J.L., van de Sanden, M.C.M and Kessels, W.M. (2010) *Journal of Applied Physics* **107**:116102 – 2010.
doi: 10.1088/0957-4484/18/49/495202.